Boiling heat transfer in narrow channels with offset strip fins: Application to electronic chipsets cooling

B. Pulvirenti, A. Matalone, U. Barucca

Accepted Manuscript

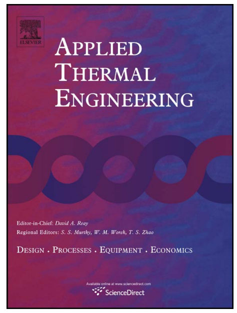

Title: Boiling heat transfer in narrow channels with offset strip fins: Application to electronic chipsets cooling

Authors: B. Pulvirenti, A. Matalone, U. Barucca

PII: S1359-4311(10)00222-X

DOI: 10.1016/j.applthermaleng.2010.05.026

Reference: ATE 3119

To appear in: *Applied Thermal Engineering*

Received Date: 15 September 2007

Revised Date: 19 May 2010

Accepted Date: 22 May 2010

Please cite this article as: B. Pulvirenti, A. Matalone, U. Barucca. Boiling heat transfer in narrow channels with offset strip fins: Application to electronic chipsets cooling, Applied Thermal Engineering (2010), doi: 10.1016/j.applthermaleng.2010.05.026

Boiling heat transfer in narrow channels with offset strip fins: application to electronic chipsets cooling

B. Pulvirenti [a]

A. Matalone and U. Barucca [b]

[a] *Dipartimento di Ingegneria Energetica, Nucleare e del Controllo Ambientale, University of Bologna, Bologna, Italy*

[b] *AAVID Thermalloy, European Headquarters, Bologna, Italy*

Abstract

An experimental study on saturated flow boiling heat transfer of HFE-7100 in vertical rectangular channels with offset strip fins is presented. The experiments have been carried out at atmospheric pressure, over a wide range of vapour quality and heat fluxes up to 1.8×10^5 W/m^2. The local boiling heat transfer coefficient has been obtained from experiments and analysed by means of Chen superposition method. Some correlations for convective boiling and nucleate boiling heat transfer coefficients have been considered. A good agreement has been found with Feldman *et al.* [3] correlation for convective boiling heat transfer and Kim and Sohn [8] correlations for nucleate boiling heat transfer.

A closed circuit for electronic chipsets cooling, with the same evaporator as that studied in the first part of the paper, has been studied. Thermal performances of this system have been measured and compared with those of a circuit with the same components but no internal fins in the evaporator. The results have shown that for high heat loads the inner geometry of evaporator does not influence the two-phase heat transfer. For low heat loads, offset strip fins evaporator gives better performances than no fins evaporator.

Corresponding author: E-mail: beatrice.pulvirenti@unibo.it

1 Keywords

Boiling heat transfer
offset strip fins
HFE-7100
electronic chipsets cooling

2 Introduction

The constant increase of packing densities and power levels of electronic devices has led to the demand of new cooling systems in the last years. In many cases, typical cooling devices based on conduction and single-phase forced or natural convection, are not more sufficient for cooling high power electronic devices. For this reason, in the last years, systems based on phase-change have been introduced in electronic cooling technology. In order to accomplish a good contact with electronic chipsets it is easier to employ heat exchangers with rectangular channels than round ducts. Then, heat exchangers with internally finned rectangular channels have been introduced as evaporators recently.

There is a wide literature on boiling and condensation heat transfer in round tubes or channels with simple cross sections, while a few works deal with channels with complex cross sections, or with internal fins. Mandrusiak *et al.* [10] studied boiling heat transfer of methanol and water inside finned channels. They obtained two-phase flow regime maps by means of visualization techniques and empirical correlations for boiling heat transfer coefficients. However, the transparent fins used for visualization were too thick to represent the actual fins. Thonon et al. [14] studied the transition between nucleate and convection boiling regimes of several fluids (R22, R113, R114 and R134a) within brazed aluminium plate fin heat exchangers. They established a criteria to characterize the transition based on the product $\mathrm{Bo} \cdot \mathrm{X}$, where Bo is the boiling number and X is the Lockhart-Martinelli parameter. Their model is not general, because takes in account the operating parameters but not the heat exchanger geometry. Feldman *et al.* [3] studied boiling heat transfer of R114 in channels with offset strip fins and perforated fins. They investigated the influence of fin dimensions in boiling regimes and proposed a semi-empirical model for predicting boiling heat transfer coefficient. Watel and Thonon [15] studied boiling heat transfer of propane within channels with offset strip fins and perforated fins. They investigated the effects of quality, mass flux, pressure and fin geometry on local convective boiling heat transfer coefficient. They did not find a good agreement between their results and correlations based on Chen superposition method [2]. They interpreted this discrepancy with the fact that boiling regime within their heat exchangers is slug-flow instead of annular flow. They did not compare their results with Carey method [1] for predicting slug flow forced convection in offset strip fins heat exchangers. An extensive review on two-phase heat transfer of hydrocarbons in compact heat exchengers and enhanced geometries may be found in Thonon [13]. Kim and Sohn [8] studied the boiling heat transfer of R113 within channels with offset strip fins. They determined experimentally the two-phase frictional multiplier as a function of the Lockhart-Martinelli parameter. Moreover, they investigated the weights of two-phase forced convective component and saturated nucleate boiling in local boiling heat transfer coefficient. They found a good agreement with a correlation based on Chen superposition method [2]. The effects of fins shapes and displacement on nucleation boiling heat transfer have been studied by Yu and Lu [16] and Ma *et al.* [9]. These Authors also found critical heat fluxes effects.

In this paper, boiling heat transfer of HFE-7100 in rectangular narrow channels with offset strip fins has been investigated.
Two main objectives have been pursued in this work. The first objective has been the experimental study of boiling heat transfer within two narrow channels with offset strip fins. A superposition method ([2], [3], [8]) has been used, in order to distinguish the contribution of nucleate boiling from convective boiling. Some correlations have been taken by the literature and discussed.
The second objective has been to design a two-phase pumped closed circuit for electronic chipsets cooling. In this circuit, boiling of HFE-7100 occurs within the evaporator in contact with the electronic chipset and the condensation occurs in an air cooled battery of tubes externally finned. Thermal performances of this device are compared with the advanced two-phase thermosyphon loop studied by Khodabandeh ([5]-[6]-[7]).
Refrigerating fluid HFE-7100 has been chosen for two main reasons.
The first reason is that this fluid is dielectric and it could be in direct contact with the electronic device. However, in the geometry shown in this paper, heater and refrigerant are not in contact, for easily changing evaporator geometries. The results obtained can be extended to equivalent systems where the refrigerant is in contact with the heater.
The second reason is that HFE-7100 has the useful property that boiling temperature is 61 °C at atmospheric pressure. Then, the cooling circuit may have a simpler design than equivalent ones with conventional refrigerants, working at much higer pressures.
In the literature there are no studies on boiling heat transfer of HFE-7100 within channels with offset strip fins.
The evaporator has two narrow channels with offset strip fins of the same geometry as that considered in the first part of the paper. Thermal resistances have been obtained experimentally and compared with those of the same circuit with the evaporator having two narrow channels with no internal fins.

3 Nomenclature

A	heat transfer area [m^2]
Bo	Boiling number
D_h	hydraulic diameter [m]
F	Reynolds number factor
g	gravity constant [9.81 m/s^2]
h	heat transfer coefficient [$W/(m^2K)$], fin height [m]
j	Colburn factor
l	fin length [m]
L	evaporator length [m]
m, $\dot{m}$	parameter defined by equation (3), mass flow rate [kg/s]
M	HFE-7100 molecular weight
Nu	Nusselt number
p	pressure [Pa]
Pr	Prandtl number
$\dot{q}$, $\dot{Q}$	heat flux [W/m^2], heat power given to the evaporator [W]
R	thermal resistance [K/W]
Re	Reynolds number
s, S	lateral fin spacing [m], nucleate boiling suppression factor
t, T	fin thickness [m], temperature [K]
U	overall heat transfer coefficient [$W/(m^2\ K)$]
v	specific volume [m^3/kg]
x	quality
X	Lockhart-Martinelli parameter
z	axial coordinate in the evaporator

Greek symbols

β	$= s/h$ dimensionless fin geometric parameter
δ	$= t/l$ dimensionless fin geometric parameter
η	fin efficiency
γ	$= t/s$ dimensionless fin geometric parameter
λ	thermal conductivity [W/(m K)]
ρ	density [kg/m^3]
μ	viscosity [kg/(m s)]
σ	surface tension [N/m]

Subscripts

a	air
b	bulk
c, cb, $cond$	critical, convective boiling, condenser
d	latent
f	fluid
g	gas
e,ev, exp	evaporator, experimental
i	inlet
l	liquid
max	maximum temperature of the surface
nb	nucleate boiling
p	primary surface
pb	pool boiling
r	reduced pressure
s, sat, sc, sp	secondary surface, saturated, sub-cooled, single phase
tp	two-phase
v	vapour
w	wall

4 Description of the experimental setup

The closed circuit investigated in this paper is shown in figure (1).

[Fig. 1 about here.]

The tested evaporator is an aluminium block with dimensions 140 mm $\times$ 250 mm $\times$ 10 mm, containing two parallel rectangular channels, each with a cross section of 3 mm $\times$ 47.5 mm and a length of 204 mm, as shown in figure (2).

[Fig. 2 about here.]

Each channel is filled with offset strip fins with dimensions $h = 2.8$ mm, $s = 2$ mm, $l = 5$ mm and thickness $t = 0.2$ mm. A sketch of offset strip fins geometry is shown in figure (3). Four thermocouples are embedded in the aluminium base of the evaporator to measure the internal wall temperature for calculation of local heat transfer coefficient. These thermocouples are useful also for detection of nucleation departure or dryout phenomena. Pressure is measured at the inlet and the outlet of the evaporator, by means of pressure transducers (Sensit HPS-A Series 4-20mA Output Pressure Transmitter, Roxspur Measurements and Control Lmtd).

[Fig. 3 about here.]

The evaporator is in contact with 36 high heat flux electronic components, simulated by an array of 6 $\times$ 6 copper blocks (hot components) with a front area of 10 mm $\times$ 10 mm and thickness 2 mm, strictly connected and heated by electric resistances. The heating power is equally distributed to the hot components and has been varied in steps from 7 to 98 W for each component. The maximum electrical power supplied to this array of hot components is $\dot{Q}_{max} = 3500$ W. The hot components simulating high heat flux sources are put in thermal contact with the evaporator through a copper layer with front area of 200 mm $\times$ 100 mm and thickness 2 mm, simulating the card support for electronic components. Since a good spread of heat has been verified through the copper layer, the maximum heat flux density obtained on the evaporator base is $\dot{q}_{max} = 1.8 \times 10^5$ W/m^2. Two thermocouples are in direct contact with the hot components, as under the copper layer two smalls grooves have been hollowed out and thermocouples have been positioned within those grooves.
The condenser is a finned bank of tubes, with four staggered rows of copper flat tubes 0.1 mm thick, with axes of 15 mm and 2 mm respectively and aluminium fins with thickness 0.2 mm. The temperatures and velocities of

external air at the inlet and outlet sections of the condenser are measured by means of thermocouples and anemometers.
Liquid flow from reservoir to evaporator is provided by a variable speed magnetic rotator with an airtight body in order to divide the rotating parts from the stator. Connections are made by transparent Rilsan ducts, with internal diameter 15 mm and thickness 1.5 mm. Mass flow rate has been obtained from volume flow rate, measured between the pump and preheater by a paddle wheel flow sensor.
Some thermocouples and pressure probes are embedded along the circuit, in order to measure the temperature and pressure distribution within the loop. All the temperatures and pressures have been registered by a data logger.

4.1 Experimental procedure and uncertainty analysis

All the measurements have been performed in steady-state. The total heating power has been varied in steps of 250 W, starting from 0 to 3500 W. The temperatures reached the steady-state typically in about 30 minutes. At the steady-state, the temperatures did not change more than 0.01 °C per minute. The uncertainty in the measurements was estimated to be ±0.1°C for the temperature, ±5% for the mass flow rate, ±2% for the pressure and ±2% for the heating power. The resulted uncertainty in heat transfer coefficient was less than ±10%.

5 Results and discussion

Single-phase heat transfer coefficient has been experimentally obtained in offset strip fins evaporator in terms of Colburn factor. The correlation obtained has been discussed, as a discrepancy with a correlation available in the literature [11] has been observed. Flow boiling heat transfer has then been studied by means of a superposition method [2]. The Colburn factor has been used for contribution of forced convection in flow boiling heat transfer, together with two correlations for Reynolds factor ([3] and [8]). The contribution of saturated nucleate boiling has been investigated by means of a pool boiling correlation weighted by Kim and Sohn suppression factor [8]. The thermal performances of the loop presented in this paper have been finally investigated, in terms of thermal resistances and overall heat transfer rate. The loop with offset strip fins evaporator has been found more efficient than a loop with the same evaporator with no fins inside the channels.

5.1 Single phase heat transfer in offset strip fins evaporator

For channels with offset strip fins, single phase heat transfer coefficient h_{sp} is given by

$$h_{sp} = \frac{\dot{Q}}{(A_p + \eta A_s)(T_w - T_b)} \quad , \tag{1}$$

where A_p and A_s are the primary and secondary surface in a channel, respectively, T_w is the wall temperature and T_b is the bulk temperature of the fluid. The fin efficiency η is given by

$$\eta = \frac{\tanh(mh)}{mh} \quad , \tag{2}$$

where h is the fin height and

$$m = \sqrt{\frac{2h_{sp}(t+l)}{\lambda t l}} \quad , \tag{3}$$

where l the fin length, t is the fin thickness and λ is the thermal conductivity of fins.
Manglik and Bergles [11] found the following correlation for air in channels with offset strip fins:

$$\begin{aligned} j &= 0.6522 \times \mathrm{Re}_{D_h}^{-0.5403}\, \beta^{-0.1541}\, \delta^{0.1499}\, \gamma^{0.0678} \\ &\times [1 + 5.269 \times 10^{-5}\, \mathrm{Re}_{D_h}^{1.34}\, \beta^{0.504}\, \delta^{0.456}\, \gamma^{-1.055}]^{0.1} \quad , \end{aligned} \tag{4}$$

where $j = \mathrm{Nu}/(\mathrm{RePr}^{1/3})$ is the Colburn factor and $\beta = s/h$, $\delta = t/l$, $\gamma = t/s$ are dimensionless characteristic parameters of the offset strip fins. In equation (4), Reynolds number is evaluated on the basis of the hydraulic diameter, defined by

$$D_h = \frac{4shl}{2(sl + hl + th) + ts} \quad , \tag{5}$$

in accord with [11]. Figure (4) shows the Colburn factor obtained from experiments (symbols) and from equation (4) (dashed line). The experimental points have been obtained with a mixture of 50 % water and 50 % ethylene glycol and with HFE-7100 in the single-phase regime.

[Fig. 4 about here.]

The figure shows that equation (4) overpredicts experimental data. This discrepancy has been observed also by Kim and Sohn [8] with R113. The Authors interpreted this disagreement between their experimental results and Manglik and Bergles [11] correlation with the fact that this correlation was obtained for gases. Gases are characterized by a smaller developing region, a lower average heat transfer rate but a higher Colburn factor. Also Hu and Herold [4] pointed out that correlations suitable for gases tend to overpredict the Colburn factor for liquids. We found the following correlation for our experimental data

$$j = 0.33\,\mathrm{Re}_{D_h}^{-0.57}[1 + 7.7 \times 10^{-5}\,\mathrm{Re}_{D_h}^{1.3}]^{0.1} \ . \qquad (6)$$

Figure (4) shows that experimental data is correlated by equation (6) with a good accuracy. Data lies within $\pm 10\%$ of equation (6) and root-mean-square error is 5 %.

5.2 Boiling heat transfer in strip-fins evaporator

In flow boiling, the overall heat transfer coefficient may still be obtained by an equation of the form (1), with T_b given by [5]:

$$T_b = \frac{T_f z_{sc} + T_{sat}(L - z_{sc})}{L} \ , \qquad (7)$$

where z_{sc} is the length of sub-cooled region, L is the evaporator length, T_f the average fluid temperature in that region and T_{sat} is saturation temperature of the fluid. For the analysis of boiling heat transfer, a pre-heating section has been used in order to have $z_{sc} = 0$. The pre-heating section has been turned off in the evaluation of thermal performances of the cooling circuit (as described in the next section).

Measured values of boiling heat transfer coefficient h_{exp} as a function of local quality x, for different fluid mass flow rates, are shown in figure (5).

[Fig. 5 about here.]

The mass flow rates measured for HFE-7100 are $\dot{m}_1 = 0.07$ kg/s, $\dot{m}_2 = 0.15$ kg/s and $\dot{m}_3 = 0.23$ kg/s. Figure shows a nucleate boiling region, for $x < 0.1$, where the heat transfer coefficient is independent on vapour quality, and a convective boiling region, for $x > 0.1$, where the heat transfer coefficient rises with vapour quality. The two regimes may be distinguished also in figure (6), where the heat transfer coefficient is plotted as a function of heat flux.

[Fig. 6 about here.]

Figure shows a region where the heat transfer coefficient is independent of heat flux (that corresponds to high values of vapour quality), and a region where the heat transfer coefficient rises with the heat flux (that corresponds to low values of vapour quality). From these results we can distinguish the nucleate boiling regime from the convective boiling regime, in accord with Feldman *et al.* [3].

The dependence of heat transfer coefficient on heat flux observed in our experiments is not very strong, in accord with Kim and Sohn [8]. They observed that it is more difficult to find a clear distinction between the nucleate boiling region and the convective boiling region in channels with offset strip fins than in round tubes. In the opinion of these Authors, the nucleate boiling on primary surface could occur simultaneously with the forced convection of liquid phase on the fins. Feldman *et al.* [3] found a strong influence of fin geometry on boiling regimes. They found that convective boiling regime is generally the dominant heat transfer mechanism for offset strip fins with a small length, while geometries with high fin length show a dominant nucleate boiling regime.
The local boiling heat transfer coefficient h_{tp} may be expressed by means of Chen superposition [2] equation

$$h_{tp} = h_{cb} + h_{nb} \ , \tag{8}$$

where h_{cb} is the convective boiling heat transfer coefficient and h_{nb} is the nucleate boiling component.
The convective heat transfer coefficient h_{cb} is related with single-phase heat transfer coefficient h_{sp} by the Reynolds factor F

$$h_{cb} = F\, h_{sp} \ , \tag{9}$$

where h_{sp} may be obtained from correlation (6), obtained in previous section. The Reynolds number factor has generally been postulated to be a function of Lockhart-Martinelli parameter X

$$X = \frac{1-x}{x}\left(\frac{f_l\,\rho_v}{f_v\,\rho_l}\right)^{0.5} \tag{10}$$

where friction factors f_l and f_v of liquid and vapour respectively have been estimated by friction factor obtained by Manglik and Bergles [11] for single-phase flow.
Figure (7) shows the Reynolds factor obtained from experiments, as a function of $1/X$ (symbols). In the figure, dashed line represents the correlation found

by Kim and Sohn [8] for offset strip fins (for $1/X > 1$)

$$F = \left[1 + \frac{2.52}{X^{0.5}} + \frac{15.1}{X^2}\right]^{0.5} , \tag{11}$$

while continuous line represents the correlation found by Feldman *et al.* [3] for offset strip fins

$$F = 1 + \frac{1.8}{X^{0.79}} . \tag{12}$$

[Fig. 7 about here.]

Figure shows that there is a better agreement between experimental data and Feldman *et al.* correlation (12) than Kim and Sohn correlation (11), for $1/X > 1$. The reason could be found in the similarity between the dimensions of fins studied in this paper and those considered in [3]. In fact, even if the height of fins used in this work is the same as that chosen by [8], fin length and fin spacing are more similar to those used by [3]. Moreover, the total length of the channels is smaller than that used in [8].
The nucleate boiling heat transfer has been evaluated by weighting with primary and secondary surface area

$$h_{nb} = \frac{h_{nb,p}\, A_p + h_{nb,s}\, \eta A_s}{A_p + \eta\, A_s} , \tag{13}$$

where $h_{nb,p}$ is the nucleate boiling heat transfer coefficient in the primary surface and $h_{nb,s}$ is the nucleate boiling heat transfer coefficient in the secondary surface. The nucleate boiling component of the local boiling heat transfer coefficient is predicted using the suppression factor S and the pool boiling proposed by Nishikawa *et al.* [12]

$$h_{nb} = S \cdot h_{pb} = S \cdot 31.4 \left[\frac{p_c^{0.2}\, F_p}{M^{0.1} T_c^{0.9}}\right] \dot{q}^{0.8} , \tag{14}$$

with

$$F_p = \frac{p_r^{0.23}}{(1.0 - 0.99\, p_r)^{0.9}} , \tag{15}$$

where p_r is reduced pressure. In equation (14), M is the molecular weight of HFE-7100, T_c is the critical temperature and $\dot{q}$ is the local heat flux. The suppression factor has been fitted by [8]

$$S = \frac{24.4}{N_b}[1 - e^{-0.041\, N_b}] , \tag{16}$$

where

$$N_b = \frac{h_{sp}}{\lambda_f}\Big[\frac{\sigma}{g(\rho_f-\rho_v)}\Big]^{0.5} , \tag{17}$$

σ is the surface tension, ρ the density and λ_f the thermal conductivity of fluid. Theoretical heat transfer coefficient h_{tp} has been finally predicted by equations (8),(9) and (13), together with correlations (12) and (16). The comparison between experimental heat transfer coefficient h_{exp} and predicted heat transfer coefficient h_{tp} is shown in figure (8).

[Fig. 8 about here.]

Figure shows that all the predicted heat transfer coefficients lies within the ±25% of the experimental results. The mean difference between the predicted and experimental heat transfer coefficient is 7 %.

5.3 Two-phase thermal performances of the closed circuit

The circuit shown in figure (1) has been employed for electronic chipsets cooling. For this application, the preheater has been turned off. The mass flow of external air at the condenser has been varied in order to achieve the better conditions for HFE-7100 at the evaporator inlet.
All the measurements shown in this section have been performed under the same boiling regimes in the evaporator as those studied in the previous section.
Thermal performances of the circuit have been obtained in terms of thermal resistances of evaporator and condenser separately and overall heat transfer coefficient of the whole circuit. These properties have been compared with those of the same circuit with the evaporator having two narrow channels with no internal fins. The results show that thermal performances of the closed loop studied in this paper are in the same range of those studied by Khodabandeh ([5]-[6]-[7]). The loop studied in this paper has more reduced dimensions thanks to the pump.

Thermal resistance of the evaporator is defined as

$$R_{ev} = \frac{T_w - T_b}{\dot{Q}} , \tag{18}$$

where T_b is the bulk temperature of the evaporator, given by equation (7). Figure (9) shows a comparison between R_{ev} of the evaporator with offset strip fins (squares) and R_{ev} of the evaporator with no fins (triangles).

[Fig. 9 about here.]

Figure (9) shows that thermal resistance of the evaporator with offset strip fins is lower than that of the evaporator with no-fins. Several experiments have been performed, by varying HFE-7100 mass flow rate. All the experiments yielded the behaiviour shown in figure (9). For $20 < \dot{q} < 80$ kW/m^2 the thermal resistance of the evaporator with offset strip fins is half the thermal resistance of the evaporator with no fins. In this range of heat loads it is very convenient to employ evaporators with offset strip fins. The difference between the two evaporators thermal resistances decreases as the heat flux rises. In fact, for high heat loads the inner geometry of evaporator gives a smaller influence on two-phase heat transfer, as observed by Feldman *et al.* [3]. These Authors observed that for high heat fluxes the nucleate boiling regime becomes dominant and under this regime the influence of fins geometry becomes negligible.
Thermal resistances in the condenser is defined as

$$R_{cond} = \frac{T_{sat,c} - T_{a,i}}{\dot{Q}} \ , \tag{19}$$

where $T_{sat,c}$ is the saturation temperature in condenser and $T_{a,i}$ is the external air temperature at the inlet section. Figure (10) shows a comparison between R_{cond} of the condenser when it is mounted in a loop with the evaporator with offset strip fins (squares) and R_{cond} of the same condenser when it is mounted in a loop with the evaporator with no fins (triangles).

[Fig. 10 about here.]

Figure shows that no relevant differences between thermal resistance of the condenser are observed for the two loops, as expected. In fact, the extended heat transfer surface of the condenser ensures a complete condensation of HFE-7100 in both the cases. We conclude that more attention should be devoted to evaporator geometry in electronic cooling design, when a two-phase closed loop like that shown in this paper is employed.

The overall heat transfer coefficient of the loop, defined by the equation

$$\frac{1}{U\,A} = \frac{T_w - T_{a,i}}{\dot{Q}} \ , \tag{20}$$

where A is the evaporator base area, is finally shown in figure (11).

[Fig. 11 about here.]

In the figure is shown a comparison between U of the loop with the evaporator with offset strip fins (circles) and U of the loop with the evaporator with no fins (triangles). Figure shows that overall heat transfer coefficient is dominated by heat transfer in the evaporator, as the same differences as those shown by figure (9) may be observed. In particular, by increasing the heat load, the difference ΔU between the two overall heat transfer coefficients changes from $\Delta U = 1.7$ W/(m^{2}K) to $\Delta U = 0.2$ W/(m^{2}K). Then, as heat load increases, a simpler geometry for the evaporator should be preferred.

6 Conclusions

In the present study, experimental investigations have been performed to analyze the flow boiling heat transfer of HFE-7100 in vertical rectangular channels with offset strip fins. Two different regimes have been detected.
The first is convective boiling regime, where heat transfer coefficient depends on quality and mass flux but is independent of heat flux. Under this regime, the correlation found by Feldman *et al.* [3], together with *ad hoc* single-phase Colburn factor, give a good agreement with our experimental results.
The second is nucleate boiling regime, with high heat flux, where the heat transfer coefficient depends on heat flux but is independent of quality and mass flux. Under this regime, correlations found by Kim and Sohn [8] give a good agreement with our experimental results.
Measured values of local flow boiling heat transfer coefficient can be predicted within $\pm 25\%$ of the correlation proposed in the present study.
As an application, thermal performances of a pumped loop for cooling of electronic chipsets have been obtained. Thermal resistances of the parts of the loop have been obtained as a function of electrical power applied to the evaporator. The comparison between two circuits with two different evaporators has shown that overall heat transfer coefficient is dominated by thermal performances of the evaporator. In particular, for heat loads higer than 120 kW/m^2 the inner geometry of evaporator gives a negligible influence on two-phase heat transfer, because the nucleate boiling regime becomes dominant, while for heat loads lower than 80 kW/m^2, the geometry of fins becomes important. In this case, particular attention should be devoted to fins geometry in electronic cooling design.

7 Acknowledgements

The auhors would like to thank Dr. Cesare Capriz for his support and useful discussions.

References

[1] V.P. Carey. Surface tension effects on convective boiling heat transfer in compact heat exchangers with offset-strip fins. *ASME Journal of Heat Transfer*, 107:970–974, 1985.

[2] J.C. Chen. Correlations for boiling heat transfer to saturated fluids in convective flow. *Industrial of Chemical Processing Designs and Devices*, 3:322–339, 1996.

[3] A. Feldman, C. Marvillet, and M. Lebouché. Nucleate and convective boiling in plate fin heat exchangers. *International Journal of Heat and Mass Transfer*, 43:3433–3442, 2000.

[4] S. Hu and K.E. Herold. Prandtl number effect on offset fin heat exchanger performance: predictive model for heat transfer and pressure drop. *International Journal of Heat and Mass Transfer*, 38:1043–1051, 1995.

[5] R. Khodabandeh. Thermal performance of a closed advanced two-phase thermosyphon loop for cooling of radio base stations at different operating conditions. *Applied Thermal Engineering*, 24:2643–2655, 2004.

[6] R. Khodabandeh. Heat transfer in the evaporator of an advanced two-phase thermosyphon loop. *International Journal of Refrigeration*, 28:190–202, 2005.

[7] R. Khodabandeh. Pressure drop in riser and evaporator in advanced two-phase thermosyphon loop. *International Journal of Refrigeration*, 28:725–734, 2005.

[8] B. Kim and B. Sohn. An experimental study of flow boiling in a rectangular channel with offset strip fins. *International Journal of Heat and Fluid Flow*, 27:514–521, 2006.

[9] A. Ma, J. Wei, M. Yuan, and J. Fang. Enhanced flow boiling heat transfer of fc-72 on micro-pin-finned surfaces. *International Journal of Heat and Mass Transfer*, 52:2925–2931, 2009.

[10] G.D. Mandrusiak, V.P. Carey, and X. Xu. An experimental study of convective boiling in a partially heated horizontal channel with offset strip fins. *ASME Journal of Heat Transfer*, 110:229–236, 1988.

[11] R.M. Manglik and A.E. Bergles. Heat transfer and pressure drop correlations for the rectangular offset strip fin compact heat exchanger. *Experimental Thermal and Fluid Science*, 10:171–180, 1995.

[12] K. Nishikawa, Y. Fujita, Y. Ohta, and S. Hidaka. Effects of the surface roughness on the nucleate boiling heat transfer over the wide range of pressure. *Proceedings of the 7th Int. Heat Transfer Conf.*, 4:61–66, 1982.

[13] B. Thonon. A review of hydrocarbon two-phase heat transfer in compact heat exchangers and enhanced geometries. *International Journal of Refrigeration*, 31:633–642, 2008.

[14] B. Thonon, A. Feldman, L. Margat, and C. Marvillet. Transition from nucleate boiling to convective boiling in compact heat exchangers. *International Journal of Refrigeration*, 20:592–597, 1997.

[15] B. Watel and B. Thonon. An experimental study of convective boiling in a compact serrated plate-fin heat exchanger. *Journal of Enhanced Heat Transfer*, 9:1–15, 2002.

[16] C.K. Yu and D.C. Lu. Pool boiling heat transfer on horizontal rectangular fin array in saturated fc-72. *International Journal of Heat and Mass Transfer*, 50:3624–3637, 2007.

List of Figures

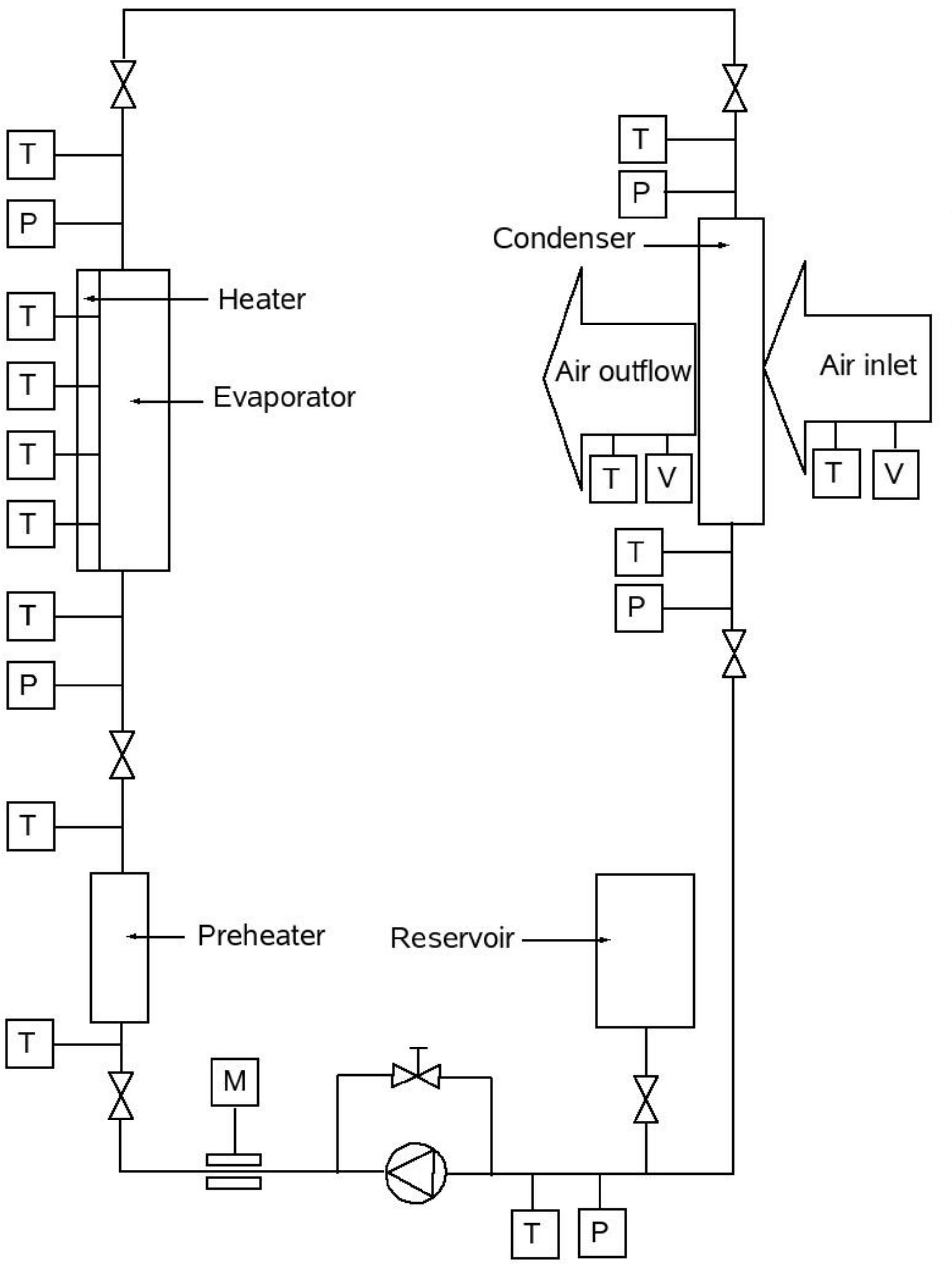

Fig. 1. Sketch of the experimental setup.

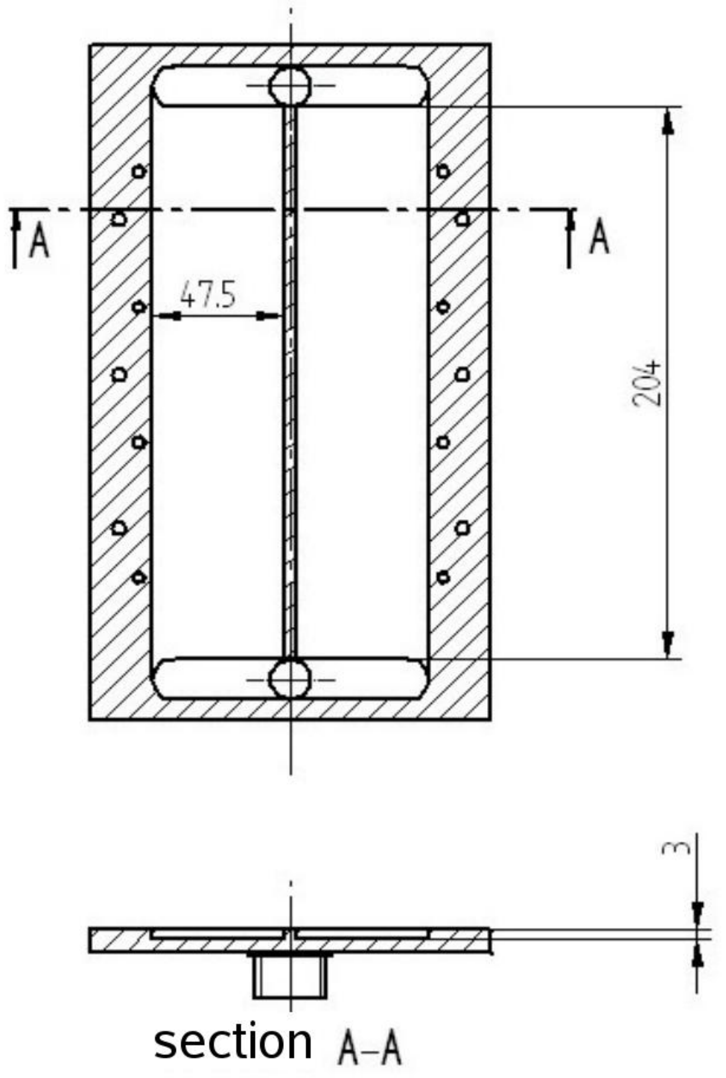

Fig. 2. Sketch of the evaporator.

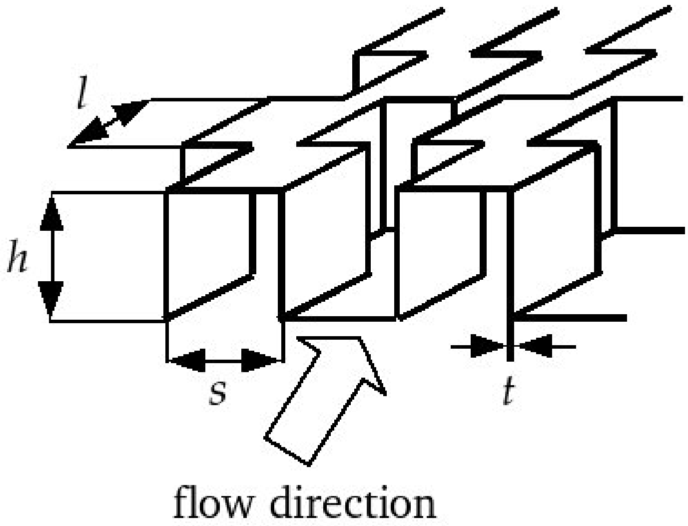

Fig. 3. Sketch of the offset strip fins geometry.

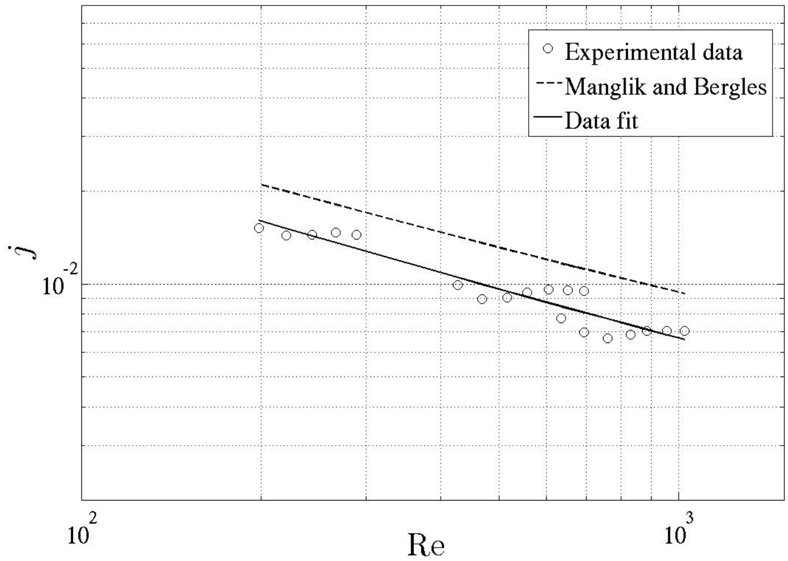

Fig. 4. Colburn factor in evaporator with offset strip fins geometry

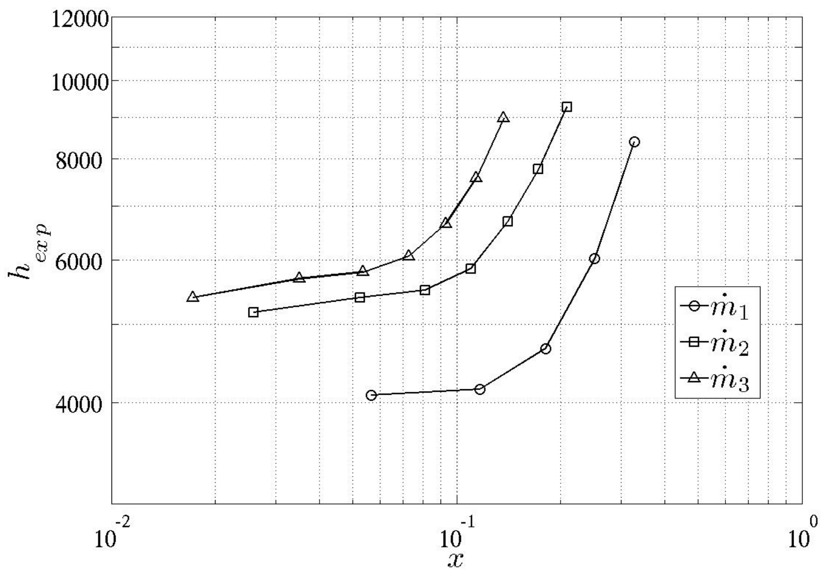

Fig. 5. Experimental boiling heat transfer coefficient [W/(m^{2}K)] in offset strip fins geometry as a function of local quality

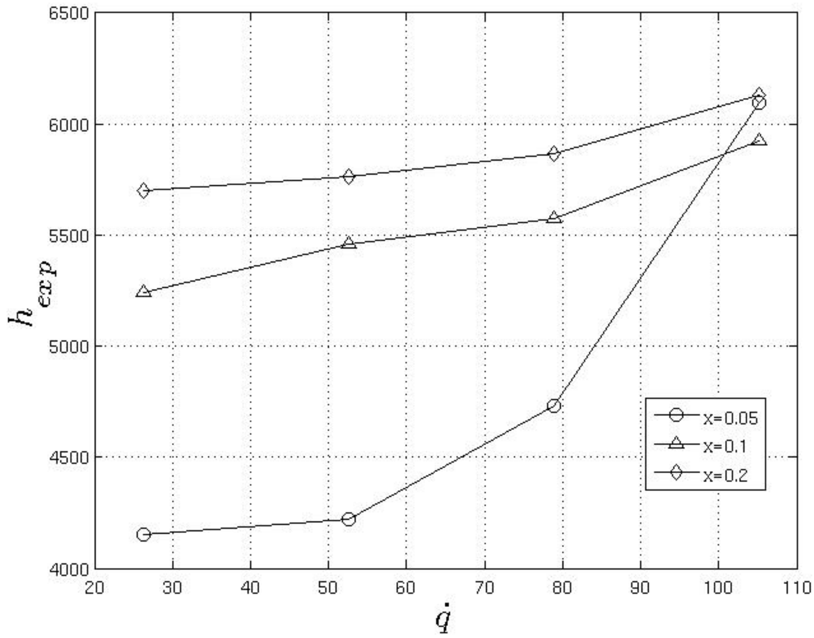

Fig. 6. Experimental boiling heat transfer coefficient [W/(m^{2}K)] in offset strip fins geometry as a function of heat flux [kW/(m^2)]

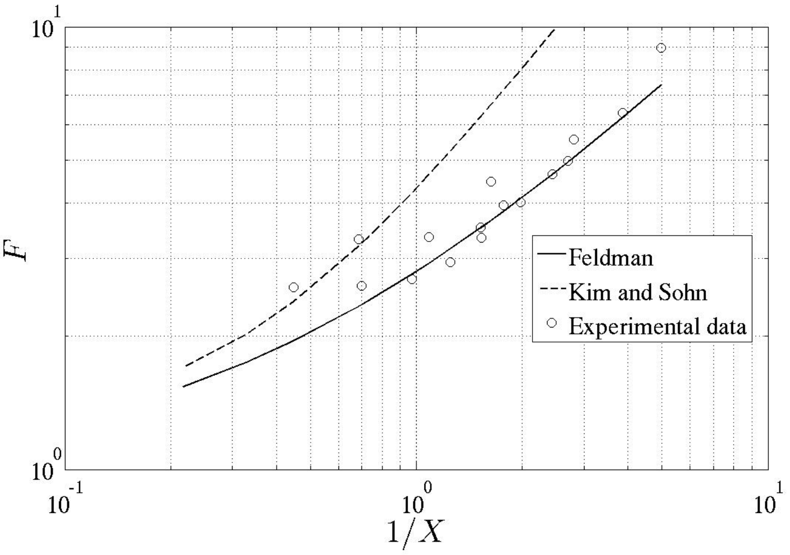

Fig. 7. Reynolds factor F obtained from experimental data (symbols) and from equations (11) (dashed line) and (12) (solid line)

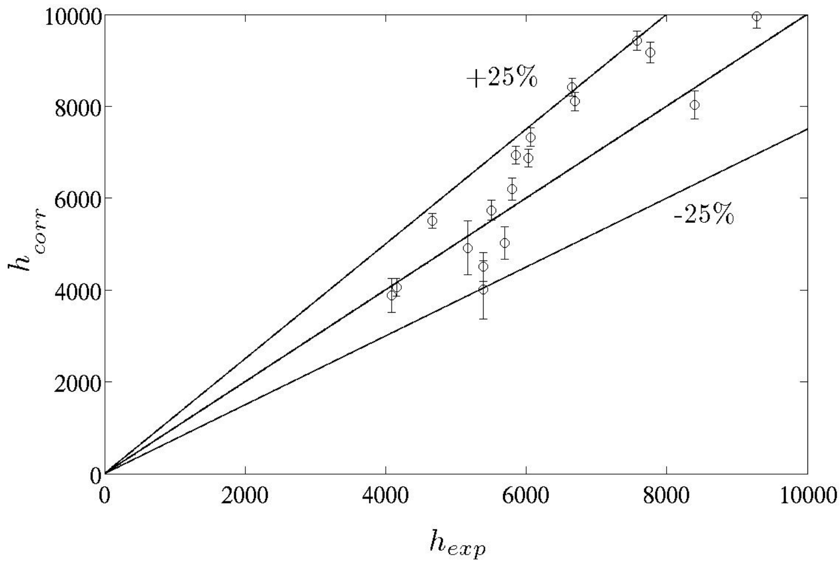

Fig. 8. Comparison of measured heat transfer coefficient with correlation (8-17) [W/(m^2 K)]

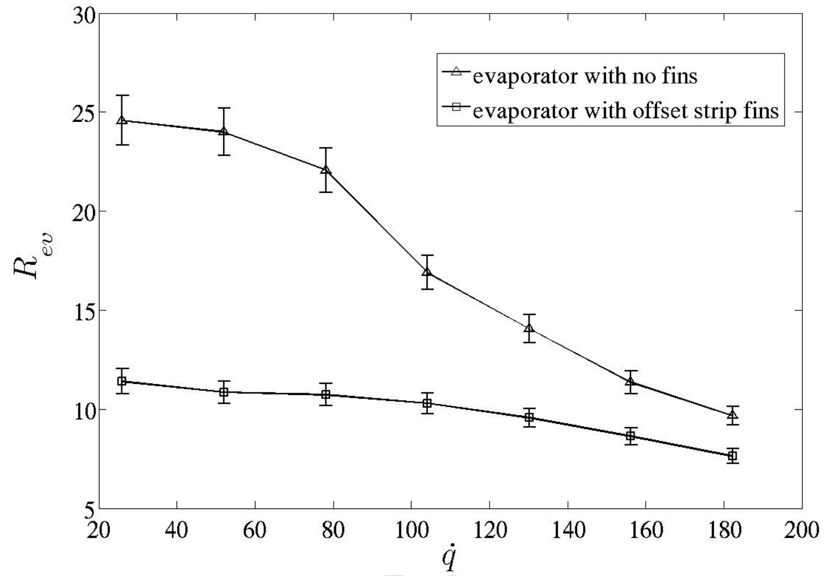

Fig. 9. Evaporator thermal resistance R_{ev} [K/kW] defined by equation (18) as a function of heat flux $\dot{q}$ [kW/m^2]. Squares and triangles represent respectively the offset strip fins and no fins evaporator.

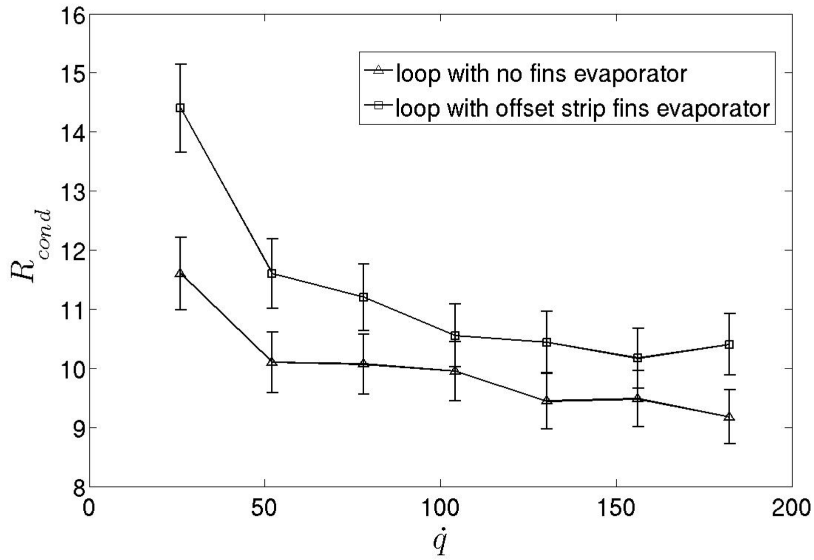

Fig. 10. Condenser thermal resistance R_{cond} [K/kW] defined by equation (19) as a function of heat flux $\dot{q}$ [kW/m^2]. Squares and triangles represent respectively the offset strip fins and no fins evaporator mounted in the loop.

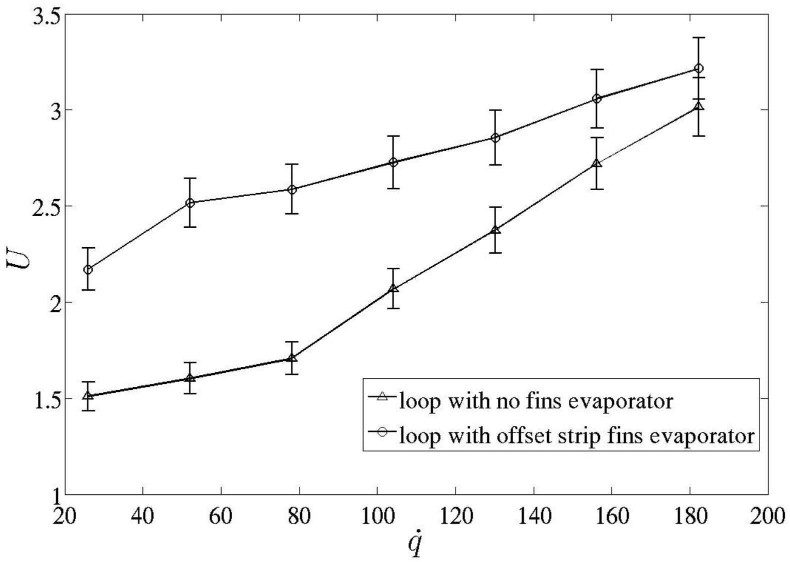

Fig. 11. Total heat transfer rate defined by equation (20) [kW/m^2 K] as a function of heat flux [kW/m^2]. Squares and triangles represent respectively the no-fins evaporator and the strip-fins evaporator.